applied sciences

MDPI

Article

Feature Analysis of Predictors Affecting the Nidus Obliteration of Linear Accelerator-Based Radiosurgery for Arteriovenous Malformations Using Explainable Predictive Modeling

Kwang Hyeon Kim and Moon-Jun Sohn *

Department of Neurosurgery, Neuroscience and Radiosurgery Hybrid Research Center, Inje University Ilsan Paik Hospital, College of Medicine, Goyang 10380, Republic of Korea
* Correspondence: mjsohn@paik.ac.kr

Abstract: This study aimed to evaluate prognostic factors associated with nidus obliteration following stereotactic radiosurgery (SRS) for cerebral arteriovenous malformations. From January 2001 to January 2018, 119 patients who underwent SRS with AVM were studied to analyze major prognostic factors (age, prescription dose (Gy), volume (mm^3), nidus size (cm), and Spetzler–Martin (SM) grade) for nidus obliteration. A random forest and tree explainer was used to construct a predictive model of nidus obliteration. The prognostic factors affecting nidus obliteration from most to least important were age, nidus size, volume, total prescription dose, and SM grade, using a predictive model. In a specific case for nidus size (1.5 cm), total dose (23 Gy), and SM grade (2), the result showed a high obliteration score of 0.75 with the actual obliteration period of 6 months spent; the mean AUC was 0.90 in K-fold cross validation. The predictive model identified the main contributing factors associated with a prognostic of nidus obliteration from linear accelerator-based SRS for cerebral AVM. It was confirmed that the results, including the prognostic factors, are potentially useful for outcome prediction for patient and treatment.

Keywords: arteriovenous malformation; explainable predictive modeling; nidus obliteration; stereotactic radiosurgery; prognostic factors

check for updates

Citation: Kim, K.H.; Sohn, M.-J. Feature Analysis of Predictors Affecting the Nidus Obliteration of Linear Accelerator-Based Radiosurgery for Arteriovenous Malformations Using Explainable Predictive Modeling. *Appl. Sci.* **2023**, *13*, 4267. https://doi.org/10.3390/app13074267

Academic Editor: Je-Keun Rhee

Received: 30 January 2023
Revised: 9 March 2023
Accepted: 22 March 2023
Published: 28 March 2023

1. Introduction

Cerebral arteriovenous malformation (AVM) is a complex cerebrovascular disorder, characterized by abnormal connections between arteries and veins that bypass the capillary bed and form high-flow, atypical arteriovenous vascular connections and shunts within the brain parenchyma. The central point of these abnormal connections is referred to as the nidus, which can range in size and complexity. The nidus is composed of an intricate network of tortuous, thin-walled vessels that are susceptible to rupture and bleeding [1]. Since brain stereotactic radiosurgery (SRS) was first introduced for AVM treatment in 1972, SRS techniques reportedly have a high AVM local cure rate. Therefore, SRS has emerged as an effective treatment that can replace the surgical treatment of cerebral AVM and can be applied to patients who cannot undergo surgery or have a high surgical risk [2,3].

The size, location, and angioarchitecture of the nidus are crucial considerations in the management of arteriovenous malformations (AVMs). These features can have a substantial impact on the risk of hemorrhage and treatment outcomes after radiosurgery. Several studies have investigated the contribution of these factors in predicting the likelihood of achieving complete nidus obliteration [4–9]. Specifically, the factors related to nidus obliteration are the presenting symptoms: whether embolization was performed before surgery; the anatomical location of the lesion; the extent of the lesion in the cerebral cortex, deep brain nucleus, or brain stem; the depth and maximal diameter of the lesion (nidus), the shape of the lesion (diffuse or compact); number of draining veins; Spetzler–Martin (SM) grade; presence of aneurysm; and presence of hematoma, among others. In the case of radiosurgery, factors related to the prescription dose (Gy) and factors such as homogeneity and conformity indexes are typically generated and evaluated during the process of radiosurgery planning have been reported as predictors of the nidus obliteration [10]. In addition, the effect of age on the prognosis of radiosurgery for AVM has been analyzed and reported. In elderly patients aged $\geq$60 years, Ding et al. investigated AVM obliteration was achieved in 66.7% population with a marginal dose of at least 22 Gy; the incidence of radiation-induced complications was minimal, and the risk of bleeding during the latent period was very low [11]. Meanwhile, Börcek et al. reported a high obliteration rate of 65.9% and low complication rate of 8.0% in pediatric AVM radiosurgery patients, based on data collected from 20 studies with 1212 patients [12]. Considering that cerebral AVMs are associated with active angiogenesis and rapid endothelial cell turnover, the treatment response to irradiation increases with younger age, and early obliteration of the nidus has been found to be related [12]. However, large-scale clinical studies have not shown any differences related to age or sex, and a clear pathological treatment mechanism caused by differences in radiation sensitivity according to age has not yet been established [13].

Several studies have analyzed various prognostic factors for outcome prediction related to successful occlusion after radiosurgery of cerebral AVM with a conventional machine learning approach [14,15]. In recent years, predictive models using artificial intelligence (AI) techniques have been used to predict the prognosis of AVM treatment. Oermann et al. (2016) reported that, by using prospective clinical data and machine learning, they obtained a specificity of 62% and a sensitivity of 85% for predicting prognosis related to occlusion of malformed vessels in SRS for cerebral AVMs [14]. Meng et al. (2022) presented results of a machine learning modeling study predicting the outcome of SRS for residual arteriovenous malformations after partial embolization [15]. For 130 AVM patients, researchers used 9 machine learning models including support vector machine (SVM), K-nearest neighbor (KNN), and neuro network (NN), and reported performance of AUC 0.66–0.78. The primary outcome was the obliteration rate, 70.77% (92 of 130), with the follow-up of 43.8 months (range, 12–108 months). A favorable outcome occurred in 89 patients (68.46%), but 41 patients (31.54%) reported an unfavorable outcome. Although an attempt was made to incorporate radiomic features in this study, in-depth feature analysis was excluded. Saggi et al., (2022) conducted a study of a machine learning model for hemorrhage prediction in pediatric patients with cerebral arteriovenous malformations [16]. Using data obtained from 186 pediatric patients, they implemented a random forest model, a gradient-boosted decision tree, and an AdaBoost model to identify features in predicting hemorrhage. Among the feature findings, gradient-boosted decision trees, AdaBoost, and random forest models showed AVM location and a concurrent arterial aneurysm as the important factors. However, the correlation of nidus obliteration based on prognostic factors has not been focused on in the conventional modeling study.

In summary, these classical machine learning research results have not explained the approach, from the perspective of correlation analysis, regarding how each studied prognostic factor contributed to the obliteration probability. Similarly, machine learning and deep learning models have been created through data training and testing, and only results for the predictability and accuracy have been reported in existing AI studies [17,18]. Therefore, these models have generally been regarded as black boxes, because it is difficult to intuitively understand the correlation or importance of factors contributing to prediction. To solve this limitation, XAI techniques have emerged in research [19].

When employing AI within the medical domain, it is crucial to ensure the dependability of the machine-generated predictions, as well as to provide comprehensive explanations of the underlying concept to users, accompanied by persuasive outcomes to support the approach. To provide explanations for the observed effects, a range of methods such as regressors, decision trees, rule-based learners, and Bayesian models may be utilized in conjunction with ensemble, support vector machines, and neural networks [18]. Predictive models, as a decision-making support system in medical practice, can, therefore, provide insights for health professionals that are improved by data-based and mathematical-based evidence [17].

Thus, this study employed explainable predictive modeling methods to investigate the prognostic potential of factors possibly linked to nidus obliteration in individuals who received cerebral AVM treatment via linear accelerator (LINAC)-based SRS. The predicted results for specific patient cases were compared to evaluate the validity of the predictive model, surpassing conventional research approaches for AVM prediction.

2. Materials and Methods

2.1. Patient Dataset

To predict nidus obliteration, data from 119 patients with AVM who underwent radiosurgery (Novalis; Varian Medical Systems, Palo Alto, CA and BrainLAB, Feldkirchen, Germany) at our institution from January 2001 to January 2018 were included in this study. Exclusion criteria were: (a) under 6 months duration of follow-up patients, (b) previous treatment SRS patients, (c) insufficient baseline data. Appropriate approval from the clinical ethics committee of our institution (Inje University Ilsan Paik Hospital, IRB No: 2019-12-016) was obtained.

In all patients, computed tomography angiography (CTA), magnetic resonance imaging (MRI) with gadolinium enhancement, magnetic resonance angiography (MRA), and trans-femoral cerebral angiography (TFCA) were used to identify and evaluate cerebral AVMs. In this study, 66 patients (55.46%) who elected for radiosurgery as a therapeutic intervention for AVM presented with SM grade III or higher, while 53 patients (44.54%) had SM grade II or lower. The selection of a treatment method was contingent upon the precise location of the AVM, with patients being carefully assessed for suitability for surgical intervention/excision or radiosurgery by board-certified neurosurgeons. When performing radiosurgery, a stereotactic head frame and equipment were used. In addition, biplanar cerebral angiography and computed tomography (CT) were combined to develop radiosurgery plan. The image delineation for nidus, feeding arteries, and draining veins were included, and radiation dose was calculated by the treatment planning system (iPlan, BrainLAB, Feldkirchen, Germany) using a 6 MV photon beam with 80% isodose line covered in total volume of nidus.

To identify the prognostic factors that affect AVM nidus obliteration, the neurosurgery department of our hospital used their existing knowledge to rank the factors that affect patient outcomes. Previously reported prognostic factors were also included in this study [20–23]. The factors selected as contributing to AVM nidus obliteration were age, total dose (Gy), AVM location (lobar or deep), AVM volume (mm^3), preoperative neurological deficits, AVM nidus size, modified AVM score, Virginia radiosurgery AVM score (VRAS), deep vein drainage, eloquent area, Spetzler–Martin (SM) grade, hemorrhage after radiosurgery, and toxicity grade. Nidus obliteration was evaluated for all patients during the follow-up period from 4 to 194 months (mean 33.4 months) by radiographic assessment including TFCA, MRA, and CTA.

2.2. Explainable Predictive Modeling

Nidus obliteration prediction was performed using a random forest classifier with a tree explainer. The correlations of each predictor and its weighted contribution to the prediction were scored by determining the Shapley additive explanations (SHAP) values (Figure 1). Our goals were to not only analyze the predictors affecting the nidus obliteration, but also predict the nidus obliteration for individual patients using a local interpretation. The performance (ROC/AUC) was evaluated using a cross validation method (Figure 1A). Figure 1B illustrates the specific modeling process for the random forest classifier. The dataset is partitioned into training and test set for prognostic factors (Xn) and a dependent variable (Y) to construct trees for prediction, using a series of pipelines. The decision outcome obtained from the trees is subsequently assessed by the test set, and a refined model is produced by means of parameter tuning including number of trees, depth of trees, and bootstrapping of the features.

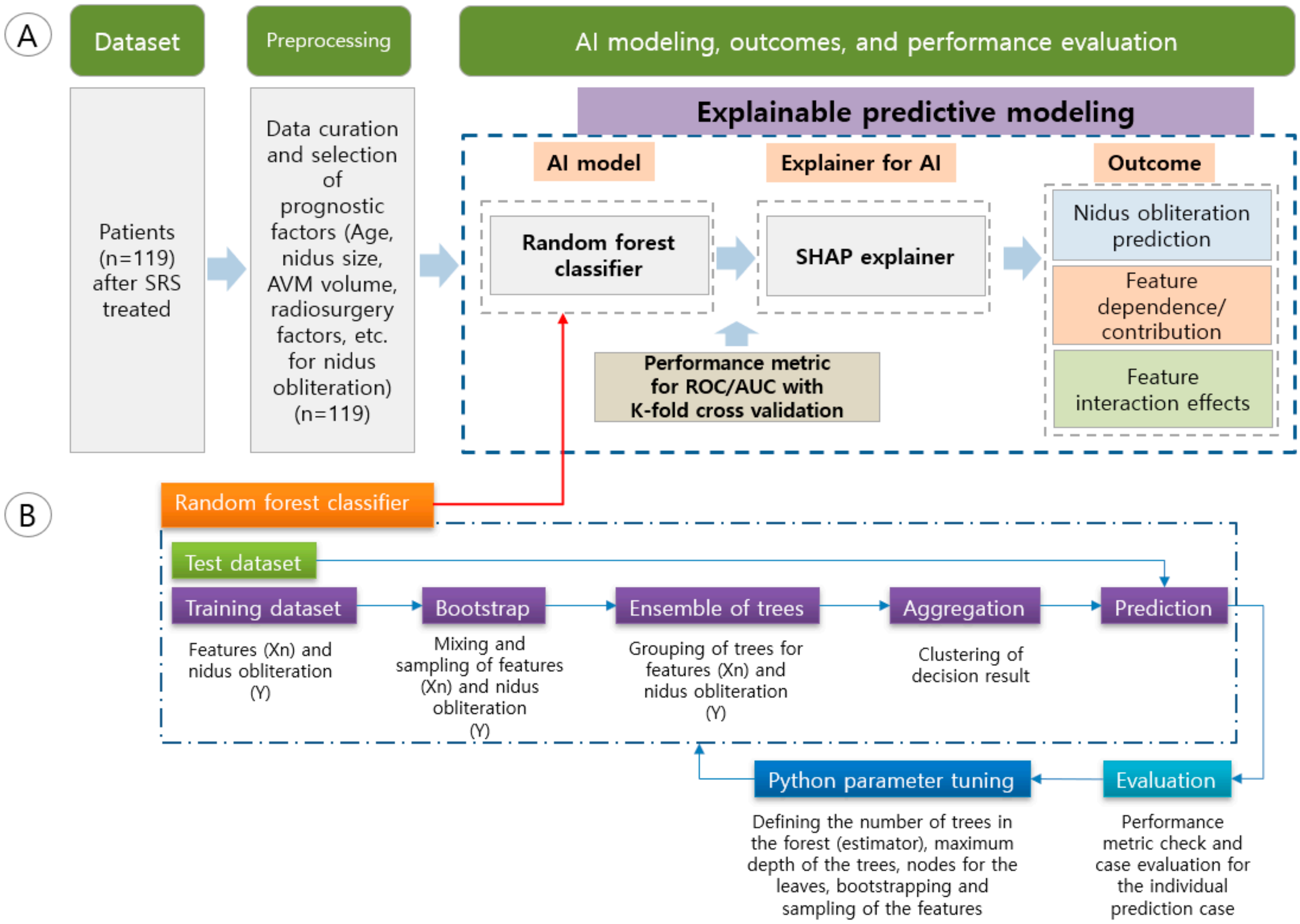

Figure 1. Diagram for nidus obliteration prediction and feature importance analysis. (**A**) Entire block diagram for the input, modeling, and output process including evaluation method. (**B**) Specific pipeline for the random forest classifier modeling process for this study.

Important factors involved in radiosurgery, such as the AVM score, deep vein drainage, eloquent area, and SM grade along with the features judged to be clinically relevant, were also analyzed for SHAP; the contributions of all prognostic factors to the SHAP predictive model were calculated by dividing the characteristics probability of each prognostic factor by the total sum of each prognostic factor influencing the outcome (Equation (1)). Therefore, the correlation between prognostic factors for nidus obliteration and the influence of each factor were shown as SHAP values [24].

$$\Phi_i(N) = \frac{1}{|N|!}\sum_R \left(v(P_i^R \cup \{i\}) - v(P_i^R) \right) \quad (1)$$

where N is the number of features, P_i^R is the set of features with order, $v(P_i^R)$ is the contribution of a set of features with order, $v(P_i^R \cup \{i\})$ is the contribution of a set of features with order i and feature i.

Random Forest is a supervised learning method that can be applied to solve classification or regression problems [25]. The method consists of a combination of tree predictors, such that each tree is independent of any vector value and uses the same layout for each vector created. For the prediction of nidus obliteration, training and testing split were conducted.

2.3. Performance Metric and Programming Environment

The ROC and AUC of the model were analyzed using K-fold cross validation. Python 3.9.12, scikit-learn 1.2.0 for predictive modeling, and SHAP 0.31.0 modules were used in the programming environment.

3. Results

3.1. Patient Characteristics Analysis

The analyzed patients' demographics are shown in Table 1. The mean age of the patients was 34 years, and 21.85% of the patients were younger than 18 years. Patients with Spetzler–Martin grade 3 or higher accounted for 55.46% of the total patient group. The mean total dose was 25.74 Gy for radiosurgery, and the mean nidus size was 2.75 cm.

Table 1. Patients' characteristics (n = 119).

Category	Unit or Sub-Category	Instance (%) or Mean ± SD
Age	years	34 ± 13
Age ≤ 18	years	26 (21.85%)
Sex	Male	82(68.91%)
	Female	37(31.09%)
Previous rupture	Yes	64 (53.78%)
	No	55 (46.22%)
Prior embolization	Yes	6 (5.04%)
	No	113 (94.96%)
AVM Location	Lobar	60 (50.42%)
	Deep	59 (49.58%)
SM grade	1	14 (11.76%)
	2	39 (32.77%)
	3	43 (36.13%)
	4	15 (12.61%)
	5	8 (6.72%)
	Median score	3
AVM Volume	mm^3	Mean 7163 (IQR Q1: 1190, Q3: 7140, min: 64, max: 15,600)
Virginia radiosurgery AVM score	0	4 (3.36%)
	1	24 (20.17%)
	2	46 (38.66%)
	3	40 (33.61%)
	4	5 (4.20%)
Modified AVM score	Median score	2.05
Deep vein drainage	Yes	51 (42.86%)
	No	68 (57.14%)
FD	Gy	20.28 ± 6.49)
Fx	Sx	102 (85.71%)
	Fx	17 (14.29%)
TD	Gy	25.74 ± 8.58
Dmax	Gy	30.02 ± 9.83
Nidus size	cm	2.75 ± 1.78

Note: SD = standard deviation; AVM = arteriovenous malformation; SM = Spetzler–Martin grade; FD = fractional dose; Fx = fraction; Sx = single fraction; TD = total dose; Dmax = maximum dose; Gy = the unit of ionizing radiation dose (J/kg).

3.2. Importance of Factor Contributions to Prediction of Nidus Obliteration

Regarding the importance of each prognostic factor affecting nidus obliteration, the specific contribution of high and low values for each factor to nidus obliteration was analyzed. A predictive model was used to analyze the contribution of each prognostic factor to nidus obliteration (Figure 2). The order of importance from highest to lowest was age, nidus size, nidus volume (mm^3), modified AVM score, total dose (Gy), SM grade, preoperative neurological deficits, and Virginia radiosurgery AVM score.

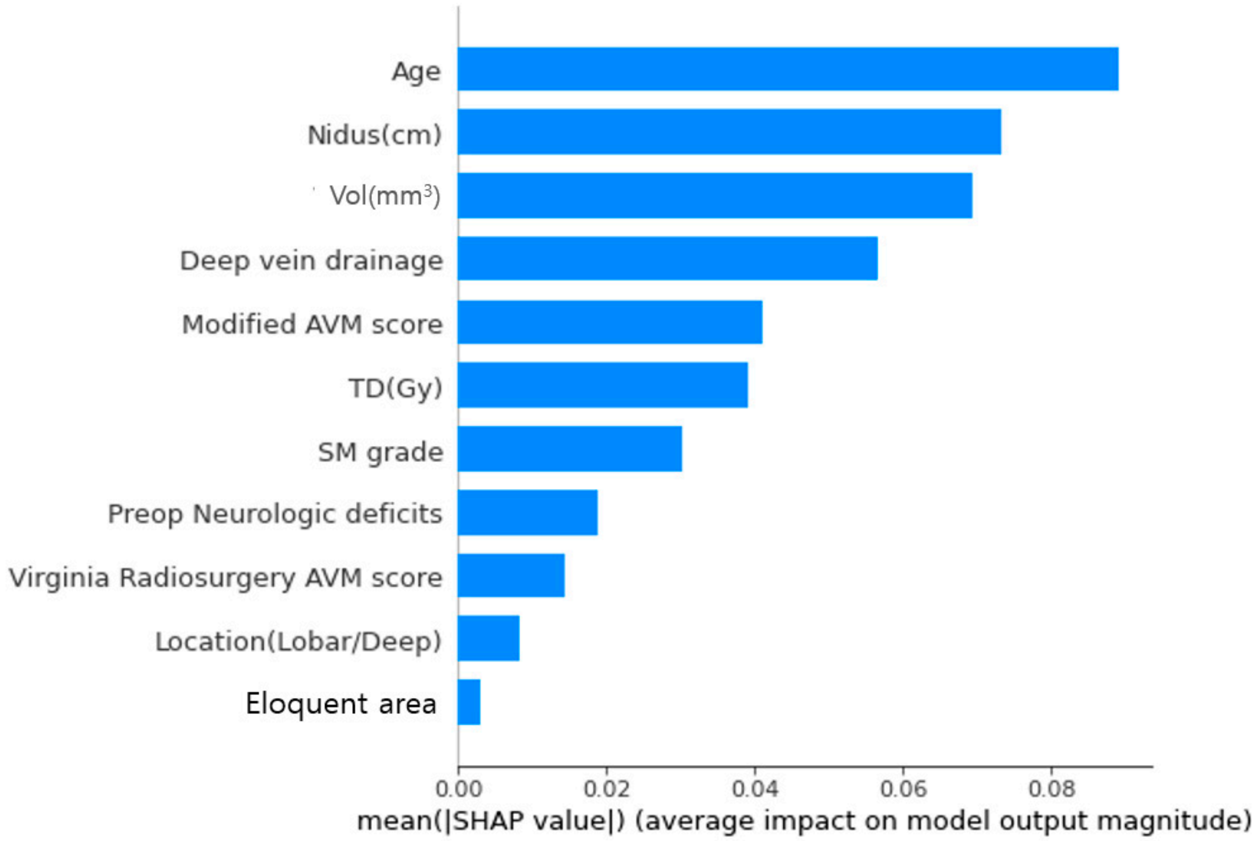

Figure 2. Feature importance for prediction of nidus obliteration.

For example, in the case of age, the mean age was 34 years and the data used for analysis showed a higher rate of obliteration in younger patients (age < 30 years). Even in the case of nidus size, patients with a size of <3 cm made a high contribution to nidus obliteration; the higher the TD (Gy), the greater the contribution to curing AVM.

3.3. Correlations between Prognostic Factors and Nidus Obliteration

The correlations between prognostic factors that mainly affected nidus obliteration were analyzed. Figure shows linearity, which means the correlation between the two groups in a specific interval. In Figure 3A, when the volume was <10 cm^3, a high total dose (Gy) was given, which was interpreted as being highly associated with nidus obliteration. In the treated patient group with nidus sizes of <3 cm, high obliteration could be expected if the nidus size was small, even in the case of age < 30 years and age ≥ 30 years (Figure 3B). In addition, the patient group with a high fractional dose and preoperative neurological deficits of severe headaches had a VRAS of <2, indicating a higher SHAP value than in the patient group with the same low score (Figure 3C,D).

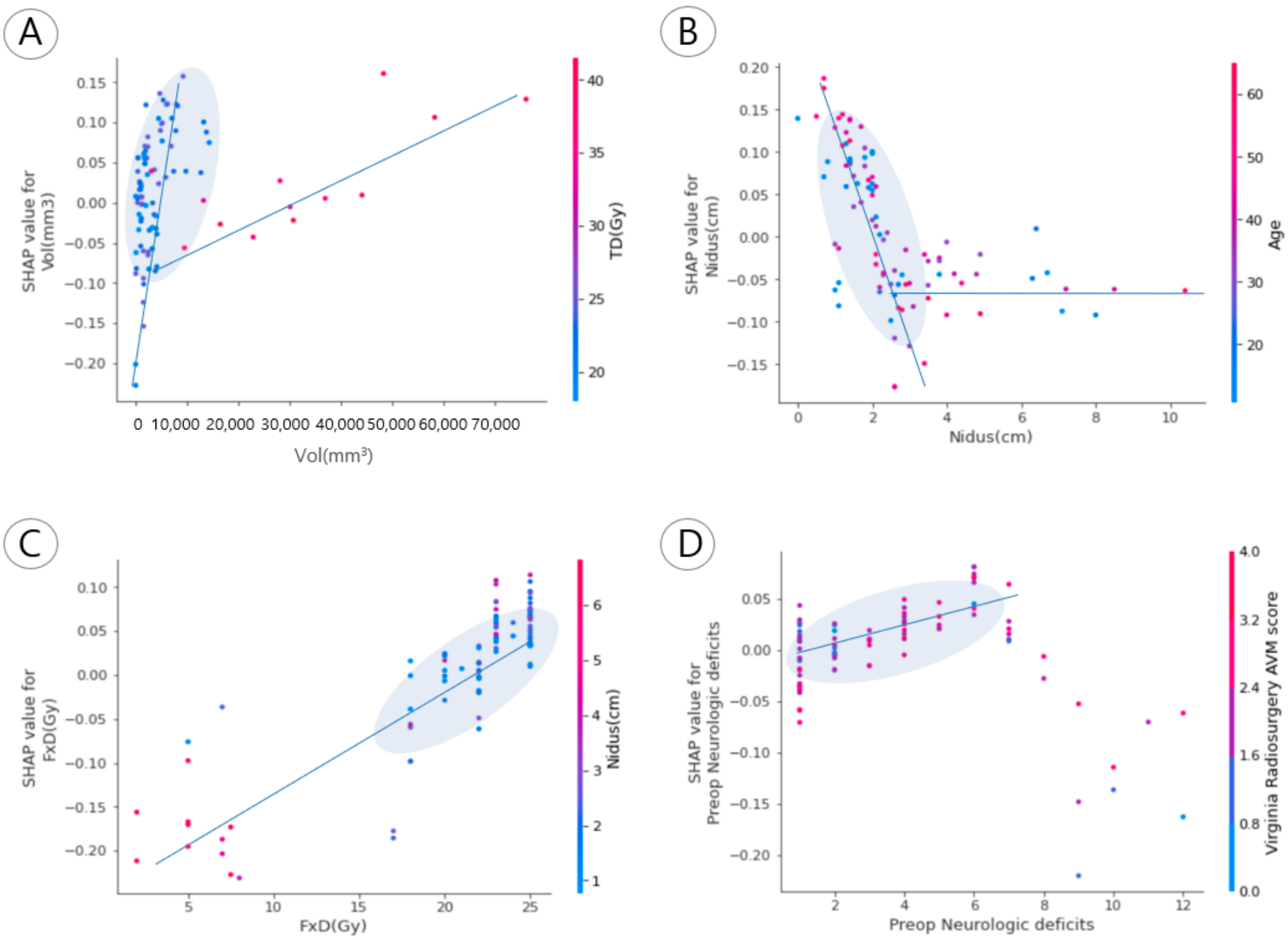

Figure 3. Factors highly associated with nidus obliteration in the correlation analysis. (**A**) Nidus volume (mm^3) vs. total dose, (**B**) Nidus size (cm) vs. age (years), (**C**) Fractional dose (Gy) vs. nidus size (cm), and (**D**) Preoperative neurological deficits vs. Virginia radiosurgery AVM score (VRAS). Note: Grey parts (dense regions of sample frequency), preoperative neurological deficit (1: headache, 2: incidental detection, 3: mental change, 4: sensory motor weakness, 5: stupor, 6: seizure, 7: dizziness, 8: syncope, 9: drowsy, 10: semicoma, and 11: diplopia), and VRAS (0–4).

Among the major factors, nidus volume and size were found to have definite effects. Two factors could be analyzed as such a result when the standard deviation is not large in the histogram of variables (Table 1). For example, the patient group with a total dose of 20–25 Gy, which did not show a large deviation, accounted for 77% of the effect on nidus obliteration, and the patient group with a volume of 76% had a volume of <10 mL (Figure 3A,B).

3.4. Individual Obliteration Probability of the Prognostic Factors

Correlations of the factors with nidus obliteration of a specific patient were plotted. In Figure 4A, the nidus volume in patient A who underwent AVM radiosurgery in our institution was 4940 mm^3, the nidus size was 3.2 cm, and the obliteration timepoint was 66 months. The SHAP value at this time showed a low value of 0.32, with a low probability of curing AVM. Additionally, B can be interpreted in the same way as A (Figure 4B). In Figure 4C, there was a relatively small volume, thus the obliteration probability was high. Specifically, in case C, the small nidus size was 1.5 cm, Spetzler–Martin grade was 2, and the obliteration date was 6 months. At this time, the SHAP value was 0.75 (Figure 4C), with a high probability for nidus obliteration. Additionally, D showed high probability for nidus obliteration due to nidus size (1.6 cm). Similarly, the factors marked in red represent areas that contributed highly to obliteration (0.85) in Figure 4D.

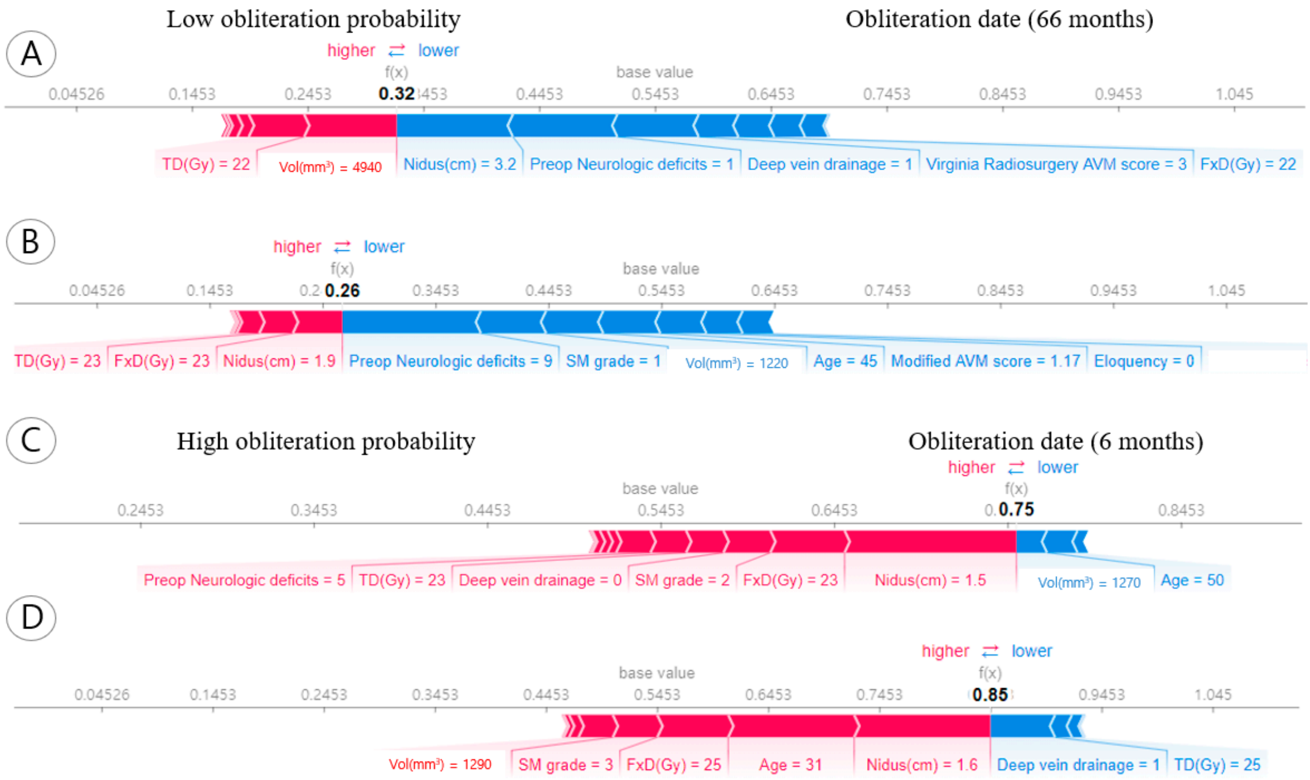

Figure 4. Nidus obliteration probability with the related clinical and dosimetric features for each patient. (**A**) For patient A, who underwent AVM radiosurgery in our institution, the nidus volume was 4940 mm^3, the nidus size was 3.2 cm, and the obliteration timepoint was 66 months (SHAP value: 0.32), with a low probability of a delay in curing AVM). (**B**) In the case of B, in which the delayed nidus obliteration was more than 60 months, the SHAP score was 0.26. (**C**) In case C, the nidus size was 1.5 cm (small), the Spetzler–Martin grade was 2, and the obliteration timepoint was 6 months (0.75, with a high probability for nidus obliteration). (**D**) Patient D showed high obliteration probability in nidus size (1.6 cm).

3.5. Partial Dependent Analysis for Nidus Obliteration

For 119 patients, the nidus size was classified in the 0.4 cm sectional range in the third, fourth, and fifth bars; the probability of correlation with nidus obliteration was then analyzed (Figure 5). The results showed that there was an obliteration probability of 76.5% for 17 patients with a nidus size ranging from 1.4 to 1.8 cm. In the case of nidus sizes ranging from 4.9 to 10.4 cm, the obliteration probability was 26.7%. The red arrow indicates the trend whereby increases in nidus size led to decreases in the obliteration probability. Overall, reasonable trends of a small nidus size increasing the probability of obliteration and of a large nidus size delaying obliteration were observed.

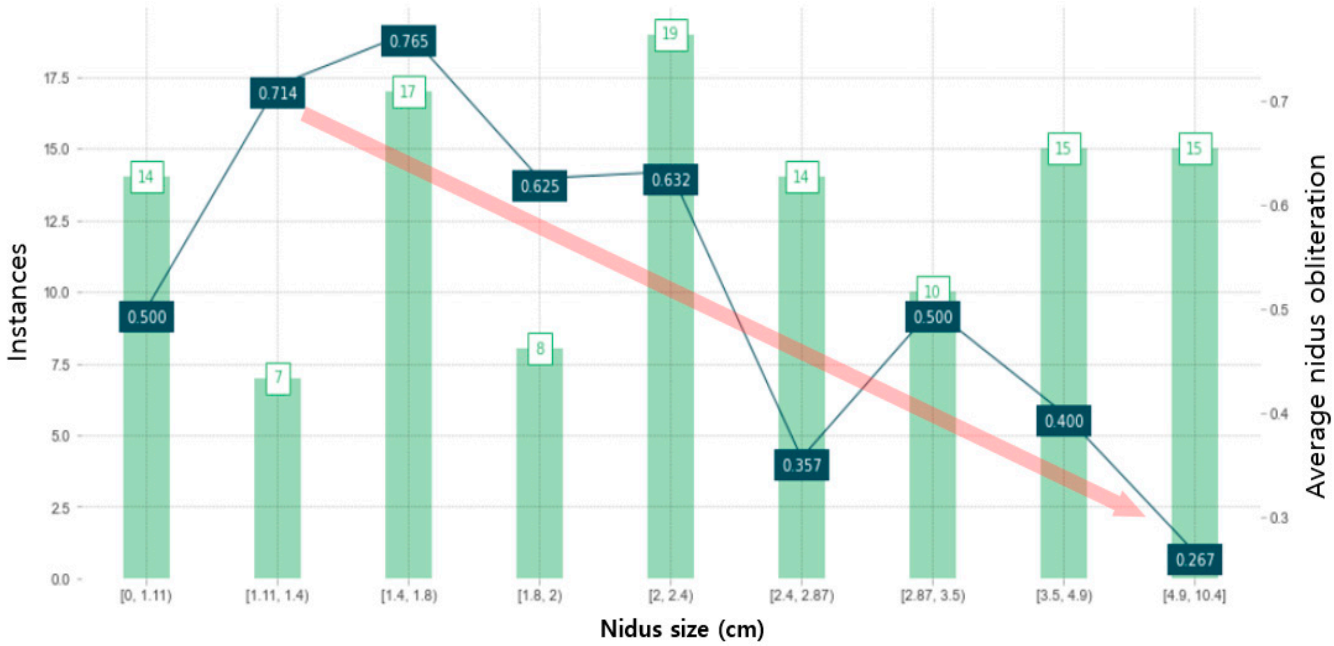

Figure 5. Relationship between nidus size (cm) and obliteration in the 0.4 cm sectional range in the third, fourth, and fifth bars. An obliteration probability of 76.5% for 17 patients with a nidus size ranging from 1.4 to 1.8 cm. In the case of nidus sizes ranging from 4.9 to 10.4 cm, the obliteration probability was 26.7%. The red arrow indicates the trend whereby increases in nidus size led to decreases in the obliteration probability.

3.6. Performance Metric

The performance metric of the model using a random forest classifier is shown in Figure 6. ROC and AUC are calculated by K-fold cross validation (K = 5). The mean AUC is 0.90 ± 0.10 in performance measurement.

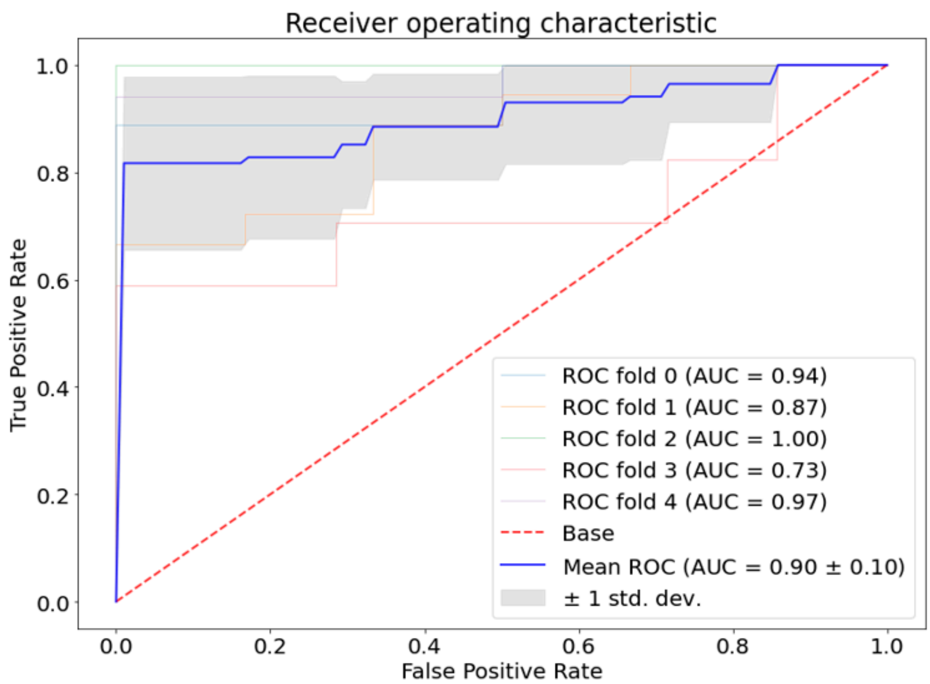

Figure 6. Performance analysis using a K-fold cross validation (K = 5). The mean AUC is 0.90 ± 0.10 in performance measurement.

4. Discussion

4.1. Prognostic Factors for Arteriovenous Malformation in Radiosurgery

An important factor in determining a local cure for cerebral AVM is nidus obliteration. We used AI modeling with various predictors to predict nidus obliteration (Table 1). Since the result in Figure 2 is shown in order of importance using a dataset that considered the patient's characteristics in our institution, the order of prognostic factors may vary depending on the patient's treatment outcome and their individual disease condition. In particular, the major clinical factors considered to be radiologically related to nidus obliteration are the extent and depth of the lesion, the maximum diameter of the lesion (nidus), number of draining veins, SM grade, presence or absence of aneurysm, and hematoma, among others [5,6,8,9,22,26]. Future research is needed because factors related to prescription dose, fractionation, and the radiation treatment plan (beam delivery method and radio-biological effect) are influential factors for radiosurgery. Furthermore, Potts et al. have examined the relationship between low marginal dose and the likelihood of AVM obliteration, as well as hemorrhage incidence, while also exploring the potential of minimizing radiosurgery-related neurological complications. These findings suggest that marginal dose could serve as a prognostic factor, warranting consideration in future research endeavors [27]. It was also found that a larger nidus volume was associated with a longer time to nidus obliteration with those probability decreased (Figure 5). This finding was consistent with the results of previous clinical studies using this partial dependence analysis for the nidus obliteration [8,9].

The major prognostic factors including the size, anatomical location, and SM grade of the lesion used by the authors are important to considered when planning radiosurgery in this study.

First, the AVM location of the lesion was 50.42% and 49.58% for lobar/deep area in Table 1; there was no significant difference in the location. That is, the location of these lesions is more related to the patient's clinical deficit, such as changes in neurological disorders, symptoms due to neurologic changes, and the risk of bleeding during the latent period, than how quickly the lesions are obliterated radiographically.

Second, it was observed that the probability of nidus obliteration of the lesion increased as the size of the nidus size decreased (Figure 5) in this study. If the size of a lesion other than AVM is considered during radiation treatment or radiosurgery, the radiation dose (Gy) to the target must be reduced in order to reduce the possibility of complications; thus, the obliteration probability is thought to decrease. Here, the determination of prescription dose for AVM treatment, which takes into account the volume and size of AVM, is contingent upon the guidelines employed by each medical institution. When the size of the AVM lesion is very large, surgical removal is often difficult. In this case, radiosurgery is the promising treatment method. However, the outcomes of radiosurgery for AVM are also decreased, and the possibility of complications (e.g., radiation toxicity) is relatively increased with increasing size. The complications after radiosurgery are known to be a major cause of brain edema, caused by radiation toxicity, and may include an increase in intracranial pressure or aggravation of neurological symptoms due to the lesion being treated. In addition, the possibility of bleeding is high as the amount of radiation is relatively small at the edge of the target lesion as age increases, accompanied by aneurysms in arteries or veins, or as the size of AVM increases [28]. In their international multicenter study, Ding et al. demonstrated that a better prognosis was observed after radiosurgery (Gamma knife) in cases with smaller-sized nidus [29]. Specifically, they found that stereotactic radiosurgery was associated with improved outcomes in patients with small, unruptured SM grade III AVM compared to those with larger or ruptured SM grade III nidus. These results are consistent with our own study's findings, which showed that smaller nidus sizes were associated with higher rates of nidus obliteration; although, the specific size of the nidus varied among the patient population (Figure 5).

4.2. Need for Explainable AI Methodology

In the field of data science, machine learning has been used as a data analysis method to overcome the limitations of big data analysis, interpretation, and statistical methods. The accuracy of a predictive model has also become a major evaluation metric that measures the prediction success or failure of research projects because various optimization models, including deep learning, are used in AI models [18,30,31]. However, since they are black boxes in which the inference results are unknown, the basis for which the prediction results were derived is unknown [32–34]. For this reason, the explainable AI (XAI) technique provides an explanatory basis for determining why a prediction result was obtained. The technique has the benefit of reducing errors that may cause future researchers to misrecognize the importance of key factors required to interpret basic statistical data. In other words, the random forest model used in this study calculated the order of importance of prognostic factors that significantly influence nidus obliteration (Figure 2). For example, the model user can see the importance of the factors affecting nidus obliteration, and it was possible to explain the differences in each important factor even for a specific patient condition (Figures 3 and 4). In addition, the authors judged that the observed trend in which nidus sizes greater than 3 cm were associated with a decreased nidus obliteration predictive value (Figure 5) was a clinically acceptable result.

However, the degree and level of acceptance for the prediction results may differ depending on the users of each institution, how they select prognostic factors contributing to obliteration, and rank their contributions. Thus, interpretation of these results may remain controversial. However, we performed several analyses attempting to solve this problem more descriptively (Figures 3–5). Through the integration of an explainer with the model employed in this study, XAI has yielded novel insights that eluded previous black box models, notably by enabling patient-specific predictions [23,35–38].

4.3. Limitation of input Data for Machine Learning Model

The characteristic of the relatively small sample size (n = 119) and the homogeneous patient population (patients of a single nationality with no racial diversity) should be addressed in the analysis outcomes. However, a cross-validation was applied for the performance validation to recognize this limitation (Figure 6). We computed and examined the significance of different features that influence the obliteration of AVM nidus using predictive modeling techniques. In addition, features with many clinical characteristics were selected as inputs such as modified AVM score and SM grade using XAI techniques; data affecting prognosis could be analyzed as an institution-specific dataset. However, as in general statistical analysis, when there is bias in the data for patients with nidus obliteration, the importance of features based on biased prediction results, such as young patients or small nidus sizes, may be distorted. For example, the idea that younger patients are more likely to experience nidus obliteration is controversial [11,39–41]. The follow-up examination of the patient's nidus obliteration involved the utilization of multiple imaging modalities, including TFCA, MRA, and CTA. This approach diverges from the use of a single uniform imaging modality and may introduce discrepancies in the interpretation of the results among readers. Additionally, the imaging data were evaluated by a team of certified neurosurgeons, potentially yielding data on both intraobserver performance and interobserver variability. Such data can be valuable in further validating the reliability and reproducibility of the results obtained. Therefore, the bias can be eliminated by using data from more cases. Furthermore, the homogeneity and conformity indexes are important factors in evaluating the characteristics of radiation irradiated to the nidus, through the evaluation of radiosurgery planning [42,43]. Therefore, these are important factors to evaluate as prognostic factors, and additional studies considering them are needed.

4.4. Expansion of Model Selection for the Outcome Analysis

In this study, an ensemble model and a tree explainer were used. However, various interpretation techniques, such as surrogate analysis, local explanation, and explainable models, can also be used [18]. Regarding deep learning applications for radiotherapy/radiosurgery, prediction of clinical outcomes is an emerging field [44].

The clinical outcome prediction was performed using the results from tracking nidus obliteration after radiosurgery in this study. Since the number of data points associated with some predictors and nidus obliteration was small, their association was not strong (Figure 2). It is feasible to make predictions using deep neural networks about the duration of obliteration for nidus size, as well as the prognosis for potential side effects such as the development of neurologic deficits, based on the location of the AVMs subsequent to radiosurgery.

5. Conclusions

The prognostic factors associated with nidus obliteration in patients with cerebral arteriovenous malformations treated with LINAC-based stereotactic radiosurgery were evaluated; their importance was assessed through predictive modeling. The analysis revealed that nidus size, volume, and total dose, along with other clinical factors, were significant predictors of obliteration. For patients with a nidus size ranging from 1.4 to 1.8 cm, the predictive model yielded a high obliteration probability of 76.5%. While the results indicate that the model can be a useful guide for patient treatment, it should be noted that more clinical factors including dosimetric factors such as marginal dose, homogeneity, and conformity indexes and a larger dataset need to be considered to improve its predictive accuracy.

Author Contributions: Conceptualization, K.H.K. and M.-J.S.; methodology, K.H.K.; software, K.H.K.; validation, K.H.K. and M.-J.S.; formal analysis, K.H.K.; investigation, M.-J.S.; resources, M.-J.S.; data curation, M.-J.S.; writing—original draft preparation, K.H.K.; writing—review and editing, K.H.K. and M.-J.S.; visualization, K.H.K.; supervision, M.-J.S.; project administration, M.-J.S.; funding acquisition, M.-J.S. All authors have read and agreed to the published version of the manuscript.

Funding: This research was funded by 2018 Inje University research grant (Grant No: 20180202).

Institutional Review Board Statement: Appropriate approval from the clinical ethics committee of our institution (Inje University Ilsan Paik Hospital, IRB No: 2019-12-016) was obtained.

Informed Consent Statement: Not applicable.

Data Availability Statement: Clinical data used in this study are approved by the IRB. Thus, data may not be used for any other purpose.

Acknowledgments: This work was supported by a 2018 Inje University research grant (Grant No: 20180202).

Conflicts of Interest: The authors declare no conflict of interest.

References

1. Lunsford, L.D.; Kondziolka, D.; Flickinger, J.C.; Bissonette, D.J.; Jungreis, C.A.; Maitz, A.H.; Horton, J.A.; Coffey, R.J. Stereotactic radiosurgery for arteriovenous malformations of the brain. *J. Neurosurg.* **1991**, *75*, 512–524. [CrossRef] [PubMed]
2. Steiner, L. Stereotaxic radiosurgery for cerebral arteriovenous malformations. *Acta Chir. Scand.* **1972**, *138*, 459–464. [PubMed]
3. Daou, B.J.; Palmateer, G.; Thompson, B.G.; Maher, C.O.; Hayman, J.A.; Lam, K.L.; Wahl, D.R.; Kim, M.; Pandey, A.S. Stereotactic radiosurgery for brain arteriovenous malformations: Evaluation of obliteration and review of associated predictors. *J. Stroke Cerebrovasc. Dis.* **2020**, *29*, 104863. [CrossRef] [PubMed]
4. da Costa, L.; Wallace, M.C.; Ter Brugge, K.G.; O'Kelly, C.; Willinsky, R.A.; Tymianski, M. The natural history and predictive features of hemorrhage from brain arteriovenous malformations. *Stroke* **2009**, *40*, 100–105. [CrossRef]
5. Hartmann, A.; Pile-Spellman, J.; Stapf, C.; Sciacca, R.; Faulstich, A.; Mohr, J.; Schumacher, H.; Mast, H. Risk of endovascular treatment of brain arteriovenous malformations. *Stroke* **2002**, *33*, 1816–1820. [CrossRef]
6. Sahlein, D.H.; Mora, P.; Becske, T.; Huang, P.; Jafar, J.J.; Connolly, E.S.; Nelson, P.K. Features predictive of brain arteriovenous malformation hemorrhage: Extrapolation to a physiologic model. *Stroke* **2014**, *45*, 1964–1970. [CrossRef]
7. Stapf, C.; Mast, H.; Sciacca, R.; Choi, J.; Khaw, A.; Connolly, E.; Pile-Spellman, J.; Mohr, J. Predictors of hemorrhage in patients with untreated brain arteriovenous malformation. *Neurology* **2006**, *66*, 1350–1355. [CrossRef]

8. Pollock, B.E.; Flickinger, J.C.; Lunsford, L.D.; Maitz, A.; Kondziolka, D. Factors associated with successful arteriovenous malformation radiosurgery. *Neurosurgery* **1998**, *42*, 1239–1244. [CrossRef]
9. Maruyama, K.; Kondziolka, D.; Niranjan, A.; Flickinger, J.C.; Lunsford, L.D. Stereotactic radiosurgery for brainstem arteriovenous malformations: Factors affecting outcome. *J. Neurosurg.* **2004**, *100*, 407–413. [CrossRef]
10. Friedman, W.A.; Bova, F.J.; Bollampally, S.; Bradshaw, P. Analysis of factors predictive of success or complications in arteriovenous malformation radiosurgery. *Neurosurgery* **2003**, *52*, 296–308. [CrossRef]
11. Ding, D.; Xu, Z.; Yen, C.-P.; Starke, R.M.; Sheehan, J.P. Radiosurgery for cerebral arteriovenous malformations in elderly patients: Effect of advanced age on outcomes after intervention. *World Neurosurg.* **2015**, *84*, 795–804. [CrossRef]
12. Börcek, A.Ö.; Çeltikçi, E.; Aksoğan, Y.; Rousseau, M.J. Clinical outcomes of stereotactic radiosurgery for cerebral arteriovenous malformations in pediatric patients: Systematic review and meta-analysis. *Neurosurgery* **2019**, *85*, E629–E640. [CrossRef] [PubMed]
13. Shin, M.; Maruyama, K.; Kurita, H.; Kawamoto, S.; Tago, M.; Terahara, A.; Morita, A.; Ueki, K.; Takakura, K.; Kirino, T. Analysis of nidus obliteration rates after gamma knife surgery for arteriovenous malformations based on long-term follow-up data: The University of Tokyo experience. *J. Neurosurg.* **2004**, *101*, 18–24. [CrossRef] [PubMed]
14. Oermann, E.K.; Rubinsteyn, A.; Ding, D.; Mascitelli, J.; Starke, R.M.; Bederson, J.B.; Kano, H.; Lunsford, L.D.; Sheehan, J.P.; Hammerbacher, J. Using a machine learning approach to predict outcomes after radiosurgery for cerebral arteriovenous malformations. *Sci. Rep.* **2016**, *6*, 21161. [CrossRef]
15. Meng, X.; Gao, D.; He, H.; Sun, S.; Liu, A.; Jin, H.; Li, Y. A machine learning model predicts the outcome of SRS for residual arteriovenous malformations after partial embolization: A real-world clinical obstacle. *World Neurosurg.* **2022**, *163*, e73–e82. [CrossRef] [PubMed]
16. Saggi, S.; Winkler, E.A.; Ammanuel, S.G.; Morshed, R.A.; Garcia, J.H.; Young, J.S.; Semonche, A.; Fullerton, H.J.; Kim, H.; Cooke, D.L. Machine learning for predicting hemorrhage in pediatric patients with brain arteriovenous malformation. *J. Neurosurg. Pediatr.* **2022**, *30*, 203–209. [CrossRef] [PubMed]
17. Tjoa, E.; Guan, C. A survey on explainable artificial intelligence (xai): Toward medical xai. *IEEE Trans. Neural Netw. Learn. Syst.* **2020**, *32*, 4793–4813. [CrossRef]
18. Arrieta, A.B.; Díaz-Rodríguez, N.; Del Ser, J.; Bennetot, A.; Tabik, S.; Barbado, A.; García, S.; Gil-López, S.; Molina, D.; Benjamins, R. Explainable Artificial Intelligence (XAI): Concepts, taxonomies, opportunities and challenges toward responsible AI. *Inf. Fusion* **2020**, *58*, 82–115. [CrossRef]
19. Gunning, D.; Stefik, M.; Choi, J.; Miller, T.; Stumpf, S.; Yang, G.-Z. XAI—Explainable artificial intelligence. *Sci. Robot.* **2019**, *4*, eaay7120. [CrossRef]
20. Mavroidis, P.; Theodorou, K.; Lefkopoulos, D.; Nataf, F.; Schlienger, M.; Karlsson, B.; Lax, I.; Kappas, C.; Lind, B.K.; Brahme, A. Prediction of AVM obliteration after stereotactic radiotherapy using radiobiological modelling. *Phys. Med. Biol.* **2002**, *47*, 2471. [CrossRef]
21. Pollock, B.E.; Storlie, C.B.; Link, M.J.; Stafford, S.L.; Garces, Y.I.; Foote, R.L. Comparative analysis of arteriovenous malformation grading scales in predicting outcomes after stereotactic radiosurgery. *J. Neurosurg.* **2017**, *126*, 852–858. [CrossRef] [PubMed]
22. Sheth, S.A.; Potts, M.B.; Sneed, P.K.; Young, W.L.; Cooke, D.L.; Gupta, N.; Hetts, S.W. Angiographic features help predict outcome after stereotactic radiosurgery for the treatment of pediatric arteriovenous malformations. *Child Nerv. Syst.* **2014**, *30*, 241–247. [CrossRef] [PubMed]
23. Senders, J.T.; Staples, P.C.; Karhade, A.V.; Zaki, M.M.; Gormley, W.B.; Broekman, M.L.; Smith, T.R.; Arnaout, O. Machine learning and neurosurgical outcome prediction: A systematic review. *World Neurosurg.* **2018**, *109*, 476–486.e471. [CrossRef]
24. Rodríguez-Pérez, R.; Bajorath, J. Interpretation of machine learning models using shapley values: Application to compound potency and multi-target activity predictions. *J. Comput. Aided Mol. Des.* **2020**, *34*, 1013–1026. [CrossRef]
25. Breiman, L. Random forests. *Mach. Learn.* **2001**, *45*, 5–32. [CrossRef]
26. Graf, E.; Schmoor, C.; Sauerbrei, W.; Schumacher, M. Assessment and comparison of prognostic classification schemes for survival data. *Stat. Med.* **1999**, *18*, 2529–2545. [CrossRef]
27. Potts, M.B.; Sheth, S.A.; Louie, J.; Smyth, M.D.; Sneed, P.K.; McDermott, M.W.; Lawton, M.T.; Young, W.L.; Hetts, S.W.; Fullerton, H.J. Stereotactic radiosurgery at a low marginal dose for the treatment of pediatric arteriovenous malformations: Obliteration, complications, and functional outcomes. *J. Neurosurg. Pediatr.* **2014**, *14*, 187–200. [CrossRef]
28. Karlsson, B.; Lax, I.; Söderman, M. Risk for hemorrhage during the 2-year latency period following gamma knife radiosurgery for arteriovenous malformations. *Int. J. Radiat. Oncol. Biol. Phys.* **2001**, *49*, 1045–1051. [CrossRef]
29. Ding, D.; Starke, R.M.; Kano, H.; Lee, J.Y.; Mathieu, D.; Pierce, J.; Huang, P.P.; Feliciano, C.; Rodriguez-Mercado, R.; Almodovar, L. Stereotactic radiosurgery for Spetzler-Martin Grade III arteriovenous malformations: An international multicenter study. *J. Neurosurg.* **2017**, *126*, 859–871. [CrossRef]
30. Rajkomar, A.; Dean, J.; Kohane, I. Machine learning in medicine. *N. Engl. J. Med.* **2019**, *380*, 1347–1358. [CrossRef]
31. Alanazi, H.O.; Abdullah, A.H.; Qureshi, K.N. A critical review for developing accurate and dynamic predictive models using machine learning methods in medicine and health care. *J. Med. Syst.* **2017**, *41*, 69. [CrossRef]
32. Sidey-Gibbons, J.A.; Sidey-Gibbons, C.J. Machine learning in medicine: A practical introduction. *BMC Med. Res. Methodol.* **2019**, *19*, 1–18. [CrossRef] [PubMed]
33. Bzdok, D.; Krzywinski, M.; Altman, N. Machine learning: Supervised methods. *Nat. Methods* **2018**, *15*, 5. [CrossRef] [PubMed]
34. Marx, V. Machine learning, practically speaking. *Nat. Methods* **2019**, *16*, 463–467. [CrossRef] [PubMed]

35. Raju, B.; Jumah, F.; Ashraf, O.; Narayan, V.; Gupta, G.; Sun, H.; Hilden, P.; Nanda, A. Big data, machine learning, and artificial intelligence: A field guide for neurosurgeons. *J. Neurosurg.* **2020**, *1*, 2688. [CrossRef] [PubMed]
36. Celtikci, E. A systematic review on machine learning in neurosurgery: The future of decision-making in patient care. *Turk. Neurosurg.* **2018**, *28*, 167–173. [CrossRef] [PubMed]
37. Buchlak, Q.D.; Esmaili, N.; Leveque, J.-C.; Farrokhi, F.; Bennett, C.; Piccardi, M.; Sethi, R.K. Machine learning applications to clinical decision support in neurosurgery: An artificial intelligence augmented systematic review. *Neurosurg. Rev.* **2020**, *43*, 1235–1253. [CrossRef]
38. Staartjes, V.E.; Stumpo, V.; Kernbach, J.M.; Klukowska, A.M.; Gadjradj, P.S.; Schröder, M.L.; Veeravagu, A.; Stienen, M.N.; van Niftrik, C.H.; Serra, C. Machine learning in neurosurgery: A global survey. *Acta Neurochir.* **2020**, *162*, 3081–3091. [CrossRef]
39. Cohen-Gadol, A.A.; Pollock, B.E. Radiosurgery for arteriovenous malformations in children. *J. Neurosurg. Pediatr.* **2006**, *104*, 388–391. [CrossRef]
40. Riva, D.; Pantaleoni, C.; Devoti, M.; Lindquist, C.; Steiner, L.; Giorgi, C. Radiosurgery for cerebral AVMs in children and adolescents: The neurobehavioral outcome. *J. Neurosurg.* **1997**, *86*, 207–210. [CrossRef]
41. Kondziolka, D.; Lunsford, D.; Flickinger, J.C. Stereotactic radiosurgery in children and adolescents. *Pediatr. Neurosurg.* **1990**, *16*, 219–221. [CrossRef] [PubMed]
42. Clement-Colmou, K.; Roualdes, V.; Martin, S.-A.; Josset, S.; Desal, H.; Campion, L.; Thillays, F. Dynamic conformal arc radiosurgery for arteriovenous malformations: Outcome and influence of clinical and dosimetrical data. *Radiother. Oncol.* **2017**, *123*, 251–256. [CrossRef]
43. Minniti, G.; Clarke, E.; Lanzetta, G.; Osti, M.F.; Trasimeni, G.; Bozzao, A.; Romano, A.; Enrici, R.M. Stereotactic radiosurgery for brain metastases: Analysis of outcome and risk of brain radionecrosis. *Radiat. Oncol.* **2011**, *6*, 48. [CrossRef] [PubMed]
44. Boldrini, L.; Bibault, J.-E.; Masciocchi, C.; Shen, Y.; Bittner, M.-I. Deep learning: A review for the radiation oncologist. *Front. Oncol.* **2019**, *9*, 977. [CrossRef] [PubMed]